UCRL--101861

DE90 000831

REACTIVE FLOW MEASUREMENTS AND CALCULATIONS FOR ZRH_2-BASED COMPOSITE EXPLOSIVES*

Michael J. Murphy, Randall L. Simpson,
R. Don Breithaupt and Craig M. Tarver
Lawrence Livermore National Laboratory
Livermore, California 94550

Cylinder test, Fabry-Perot laser interferometric and detonation velocity-charge diameter experiments were done to determine the detonation reaction zone structures and reaction product equations of state of a family of HMX/AP/ZrH_2/estane explosives. This experimental data base is used to develop ignition and growth reactive flow models of the detonation waves in these composite explosives. The experiments and calculations clearly demonstrate the Zeldovich-von Neumann-Doering (ZND) structure of the detonation reaction zones which are several millimeters long. The inferred reaction rates imply that the HMX in these formulations reacts first at rates comparable to those measured in other HMX-based explosives and propellants. The remaining components of these explosives then decompose at much slower rates. However, this decomposition is rapid enough to contribute to the propagation of the detonation wave and to the total energy delivered in metal acceleration applications.

INTRODUCTION

Composite or non-ideal explosives are mixtures in which the fuel (carbon and/or hydrogen rich) and oxidizer (oxygen and/or fluorine rich) are separated either partially or completely in distinct molecules and/or phases. Theoretically, if all of the oxidizer atoms are able to diffuse to and react with fuel atoms, composite explosives can liberate significantly more energy than monomolecular explosives during metal acceleration and other applications. The desire to understand and control the reaction kinetics of energy release in composite explosives has driven a long term study[1–6] of the effects of particle size, elemental composition, reaction zone temperature and pressure, and other initial conditions on the performance of this class of explosives.

The basic experimental tool used to measure the relative energy release of composite versus monomolecular explosives as a function of time has been the cylinder test, in which a copper wall is accelerated radially outward by the detonating explosive. The copper wall velocity is continuously recorded by streak cameras and in recent years by Fabry-Perot laser interferometric techniques. The detonation velocity and sometimes the detonation pressure are also measured. The main theoretical analysis has been to fit the wall velocity history with a Jones-Wilkins-Lee (JWL) reaction products equation of state assuming that a Chapman-Jouguet (CJ) detonation had been established. Approximate analyses, such as those recently published by Doherty *et al.*,[7,8] have also been developed for relative energy release estimations at certain volume expansions of the explosive products.

Several nanosecond time resolved experimental techniques and reactive flow computer code models are currently being used to measure and calculate the detonation reaction zones and overall energy delivery of monomolecular and composite explosives. Embedded pressure and particle velocity gauges and

*Work performed under the auspices of the U.S. Department of Energy by the Lawrence Livermore National Laboratory under Contract W-7405-Eng-48.

VISAR and Fabry-Perot laser interferometric techniques have been widely applied to measure the reactive flows produced during shock initiation and detonation of monomolecular explosives.[9-16] In addition to confirming the hot spot mechanism of shock initiation and the Zeldovich-von Neumann-Doering (ZND) structure of detonation waves, these experimental records provide the quantitative information required to develop reactive flow computer models, such as the ignition and growth model,[17] which can then be used to predict the explosive's response in other scenarios. In this paper and a related one,[18] these experimental techniques and reactive flow modeling are applied to families of composite explosives and propellants to determine the detonation reaction zone structures of these multicomponent materials. In this paper composite explosives containing HMX, ammonium perchlorate (AP), ZrH_2 and an estane binder are studied in cylinder tests, one-dimensional Fabry-Perot laser interferometric experiments, and detonation velocity as a function of charge diameter experiments to determine their energy release rates under several conditions for reactive flow model development.

EXPLOSIVES AND EXPERIMENTS

The HMX/AP/ZrH_2/binder family of explosives, designated as RX-25-xx, was developed for applications requiring relatively high density, high energy and low detonation velocity explosives. Two main formulations, RX-25-BH and RX-25-BF, were used in this study. RX-25-BH contains 19% by weight HMX (Class A particle size), 47% AP (5 micron particle size), 30% ZrH_2 (Class F particle size) and 4% estane binder. RX-25-BH is pressed to a density of 2.30 g/cm^3 (98.3% TMD) and has a detonation velocity of 6.01 mm/μsec. RX-25-BF contains 38% by weight HMX (Class A particle size), 36% AP (5 micron particle size), 22% ZrH_2 (Class F) and 4% estane binder. RX-25-BF is pressed to 2.149 g/cm^3 (98.2% TMD) and has a detonation velocity of 7.506 mm/μsec. Two particle size variations of this 38% HMX formulation were also used in some of the experiments: RX-25-BP (LX-04 grade HMX, 8 micron AP) and RX-25-BQ (6 micron HMX, 8 micron AP). While these particle size variations affect the formulation and shock initiation properties, they do not have significant effects on the detonation experiments done in this study.

These detonation experiments include: five cylinder tests, eight Fabry-Perot laser interferometry shots and two critical diameter-detonation velocity measurements. Three standard cylinder tests with 50 mm diameter explosive charges driving 2.54 mm thick copper walls were fired using RX-25-BH, RX-25-BF and RX-25-BP. Two other cylinders were fired using 25 mm diameter RX-25-BF charges, one with a 1.27 mm thick copper wall and one with a 2.54 mm thick copper wall. The 25 mm diameter cylinder test velocity histories scaled with those obtained in the 50 mm diameter shots indicating that the 38% HMX formulations release their energy nearly identically at these diameters. Since two streak records are taken per cylinder test, eight wall velocity histories are available for the 38% HMX formulations. Fabry-Perot laser interferometry was available for the most recent cylinder test on RX-25-BP, and the two Fabry-Perot velocity histories closely agree with the streak camera records when the required corrections for copper wall angle directions are made.[19] The one-dimensional Fabry-Perot shots consist of: a 0.254 mm thick Mylar flyer plate accelerated to 4.3 mm/μs by an electric gun, a 3 mm thick LX-10 booster pellet, a 12.6 mm or 25.5 mm thick RX-25-BH, BF, BP or BQ pellet, and a LiF crystal coated with 4000 Å of gold to provide a reflecting surface. The Fabry-Perot laser interferometer thus measures the particle velocity history of the explosive—LiF interface. The LX-10 boosters were added to insure RX-25 detonation, but Fabry-Perot records taken without the LX-10 booster pellet showed no effects of the shock initiation process in the RX-25 explosives. The two critical diameter-detonation velocity experiments consisted of SE-1 detonators igniting tetryl pellets which in turn initiated LX-17 pellets (TATB was used for close CJ pressure matching to RX-25-BP) and finally either 6.4 mm diameter or 12.7 mm diameter charges of RX-25-BP. The 6.4 mm diameter RX-25-BP charge was 32 mm long and piezoelectric crystal pins were placed 6.3 mm apart to measure detonation velocity. The 12.7 mm diameter RX-25-BP charge was 63.6 mm long with shorting switches every 12.7 mm to measure detonation velocity.

This combination of three experimental tests yields one-dimensional detonation reaction zone structure and early product expansion histories, the two-dimensional effects of finite charge diameters on reaction zone structure and the two-dimensional overall energy delivery to an expanding metal wall. Although ideally one should obtain as much experimental data as possible, this amount of data is sufficient to develop a useful reactive flow computer model of these detonating explosives.

REACTIVE FLOW MODEL DEVELOPMENT

A reactive flow hydrodynamic computer code model for a monomolecular explosive requires: an

unreacted explosive equation of state, a reaction product equation of state, a reaction rate law that governs the chemical conversion of explosive molecules to reaction product molecules, and a set of mixture equations to describe the states attained as the reactions proceed. The unreacted equation of state is normalized to shock Hugoniot and von Neumann spike state detonation data. The reaction product equation of state is normalized to expansion data, such as that obtained in a cylinder test. The reaction rates are inferred from embedded gauge and/or laser interferometric measurements of pressure and/or particle velocity histories. Ideally, for multicomponent composite explosives, each component's unreacted and product equations of state and all of the possible reaction rates should be modeled, as discussed by McGuire and Finger.[6] Such detailed models have been implemented in the DYNA2D hydrodynamic code.[20] However, as is the case with these HMX/AP/ZrH_2/estane explosives, the equations of state for all of the individual components have not been measured and the experimental data has been obtained on the composite explosive formulations. Therefore the available unreacted and product equations of state are those of the explosive mixture.

The measured reaction rates are also "composites" for the whole mixtures. However, for systems whose individual components react at different rates, the reaction rate laws in the ignition and growth model have been used to describe the sequential or simultaneous decomposition of individual components. This treatment has successfully calculated experimental data on RX-26-AF,[21] which is half HMX and half TATB, and various HMX-based propellants.[18] For RX-25-BH and RX-25-BF, the reaction rates calculated for the HMX-based explosives PBX-9404 and LX-14[17] are used to model the initial decomposition of 19% in RX-25-BH and 38% in RX-25-BF, because the HMX in these formulations reacts first. Then, since the decomposition rates of ZrH_2 and AP and the rates of any diffusion controlled reactions between reaction product molecules at these temperatures and pressures are unknown, the remainder of the energy release is modeled as a single term in the ignition and growth reaction rate law.

Table 1 contains the equation of state, reaction rate law coefficients, and detonation parameters for RX-25-BH and RX-25-BF used in this paper. The unreacted and product equations of state are both JWL (i.e., Gruneisen) forms

$$p = Ae^{-R_1V} + Be^{-R_2V} + \frac{w\,C_vT}{V} \qquad (1)$$

where p is pressure, V is relative volume, T is temperature, and A, B, R_1, R_2, w (the Gruneisen coefficient) and C_v (the average heat capacity) are constants. The ignition and growth reaction rate law is of the form:

$$\frac{\partial F}{\partial t} = I(1-F)^b\,(r/r_0 - 1 - a)^x$$

$$+ G_1(1-F)^c\,F^d\,p^y + G_2\,(1-F)^e\,F^g\,p^z \qquad (2)$$

where F is the fraction reacted, t is time, r_0 is initial density, r is current density, p is pressure in Mbars, and I, G_1, G_2, b, x, a, c, d, y, e, g, and z are constants. The first rate is the hot spot ignition term and is set equal to zero when F exceeds Figmax. Since the amount of explosive ignited by the shock front has been experimentally demonstrated to be approximately the initial void volume, Figmax is set equal to 0.03 because the RX-25-BH and RX-25-BF were pressed to 97–98% TMD. The second rate describes the growth of the ignited hot spots and the HMX rates previously published[17] are used until F exceeds F_{G1max} (0.19 for RX-25-BH and 0.38 for RX-25-BF). The third rate models the completion of reaction for $F_{G1max} \le F \le 1$. The comparisons between the experimental records and the corresponding reactive flow calculations are shown in the next section.

COMPARISONS OF EXPERIMENTS AND CALCULATIONS

1) RX-25-BH (19% HMX) FORMULATIONS

One cylinder test and two Fabry-Perot experiments using 2.55 cm lengths of RX-25-BH boosted by 0.3 cm of LX-10 were performed. Figure 1 shows the comparison of the average of the two streak camera experimental records of the copper wall velocity history with the hydrodynamic code calculations assuming a CJ detonation using the product equation of state listed in Table 1 and a ZND reactive flow detonation using all of the parameters listed in Table 1. This average experimental record agrees more closely with the ZND reactive flow calculation at early times (less than five microseconds) and then with the CJ detonation calculation at later times. The late time agreement with the ideal CJ calculation occurs because the product JWL equation of state is fitted to the overall energy and momentum produced by the entire expansion process. Thus this product equation of state includes some of the momentum produced in the finite thickness reaction zone of RX-25-BH but delivers it to the cylinder wall at later times. When a finite thickness reaction

TABLE 1. EQUATION OF STATE AND REACTION RATE PARAMETERS FOR RX-25-BH AND RX-25-BF.

Explosive	RX-25-BH		RX-25-BF	
JWL Parameters	Unreacted	Products	Unreacted	Products
A (Mbars)	286.9	20.62243	286.9	53.24
B (Mbars)	−0.1453	0.2867773	−0.1453	0.5140
R_1	10.0	7.0	10.0	8.0
R_2	2.0	1.0	2.0	1.75
ω	0.8161	0.6	0.8161	0.6
C_v (Mbars/K)	2.7298×10^{-5}	1×10^{-5}	2.7298×10^{-5}	1×10^{-5}
T_0 (°K)	298	—	298	—
E_0 (Mbar-cc/ccg)	—	0.08	—	0.100
CJ State Parameters				
ρ_0 (g/cm^3)	—	2.300	—	2.149
D (mm/μs)	—	6.010	—	7.506
p_{CJ} (Mbars)	—	0.210	—	0.280
ρ_{CJ}/ρ_0	—	0.7472	—	0.7687
u_{CJ} (mm/μs)	—	1.519	—	1.736
Reaction Rate Parameters				
I (μs^{-1})	7.43×10^{11}		7.43×10^{11}	
b	0.667		0.667	
a	0.0		0.0	
x	20.0		20.0	
G_1 (Mbars^{-y} μs^{-1})	3.1		3.1	
c	0.667		0.667	
d	0.111		0.111	
y	1.0		1.0	
G_2 (Mbars^{-z} μs^{-1})	85.0		25.0	
e	0.667		0.667	
g	0.111		0.111	
z	2.0		1.2	
Figmax	0.03		0.03	
F_{G1max}	0.19		0.38	

zone is known to be present, more recent product JWL equations of state are based on lower CJ pressures and initial energies.

The presence of a reaction zone induced higher initial wall velocity is not seen in Fig. 1 which contains only the average of the two streak camera records. One of the two camera records did record initial velocities of 0.8 mm/μs or higher. When Fabry-Perot laser interferometry or a similar technique is used to measure the initial velocity, the von Neumann spike state is easily observed. Figure 2 compares two experimental velocity histories of the interface between detonating RX-25-BH and LiF to two hydrodynamic code calculations, one assuming an ideal CJ detonation of RX-25-BH and the other a reactive flow calculation of the shock initiation and subsequent detonation of RX-25-BH. Since the Fabry-Perot technique has a time resolution of a few nanoseconds, most of the detonation reaction zone is observed, as demonstrated by the measured initial velocities of 1.5–1.6 mm/μs in Fig. 2 compared with the 1.37 mm/μs predicted by the ideal CJ calculations. The ZND reactive flow calculation agrees with the measured initial velocities in Fig. 2. The predicted time for complete reaction of RX-25-BH at the LiF interface is approximately 0.4 μs, and the

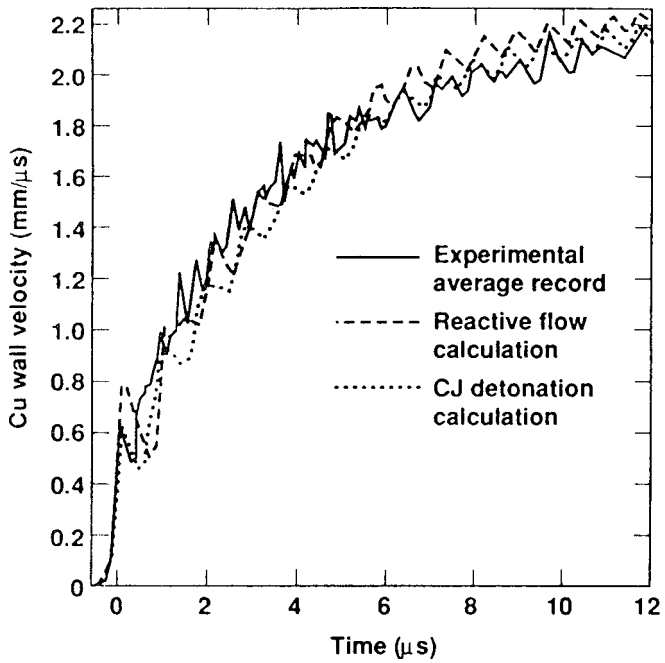

FIGURE 1. COMPARISON OF AVERAGE EXPERIMENTAL RECORDS AND CALCULATIONS OF THE COPPER CYLINDER WALL VELOCITY HISTORY PRODUCED BY DETONATING RX-25-BH.

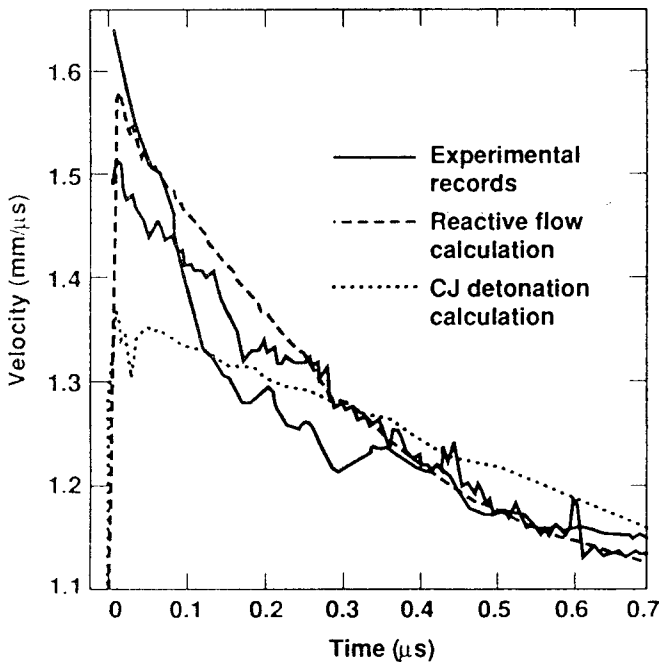

FIGURE 2. EXPLOSIVE-LIF WINDOW INTERFACE VELOCITY HISTORIES PRODUCED BY 2.55 CM OF DETONATING RX-25-BH.

reactive flow calculation agrees very closely with both experimental records from 0.4 μs to the end of the records in Fig. 2. Both the reactive flow calculation and the experimental velocities in Fig. 2 are less than those predicted by an ideal CJ detonation at times greater than 0.4 μs. This implies that the RX-25-BH detonation wave has not yet attained its final ZND structure after only 2.55 cm of propagation. This has been previously observed for explosives which exhibit detonation reaction zone lengths of several tenths of a microsecond, such as triaminotrinitrobenzene (TATB)-based explosives.[22] Experiments using longer charges are required to resolve this matter. However, this reactive flow model for RX-25-BH is certainly useful for estimating most of its detonation properties. The calculation predicts that the first 19% of reaction occurs in approximately 60 ns and its predicted particle velocity decrease in the first 60 ns agrees closely with experiment, as shown in Fig. 2. This justifies the use of the HMX reaction rates for the first 19% of the reaction. A better understanding of the reaction rates of the remaining explosive components and the approach to a sonic or CJ-like state requires more experiments and further modeling.

2) RX-25-BF (BP, BQ)—38% HMX FORMULATIONS

As previously mentioned, four cylinder tests have been fired using RX-25-BF and BP. The streak camera records for these four shots (eight in all) agree quite closely. The most recent cylinder test also yielded two Fabry-Perot wall velocity histories. Figure 3 compares the average Fabry-Perot velocity history (corrected to slit velocity), the average streak camera velocity history, the reactive flow calculated wall velocity history and the CJ detonation calculated wall velocity history. Both experimental techniques show the effect of the finite thickness reaction zone (several of the eight individual streak camera records show initial velocities as high as 1.4 mm/μs) and agree more closely with the reactive flow calculation than the CJ detonation calculation.

Six one-dimensional Fabry-Perot laser interferometric experiments using LiF windows were run on detonating RX-25-BF, BP and BQ. One experiment had a 3 mm thick LX-10 booster and only 12.6 mm of RX-25-BF. The measured explosive—LiF interface velocity is shown in Fig. 4 along with the CJ detonation and reactive flow calculations. The experimental presence of a developing von Neumann spike state is clearly observed in Fig. 4, although it is slightly below the reactive flow calculation. The ideal CJ calculation underestimates the momentum produced in this experiment. Five Fabry-Perot experiments were shot

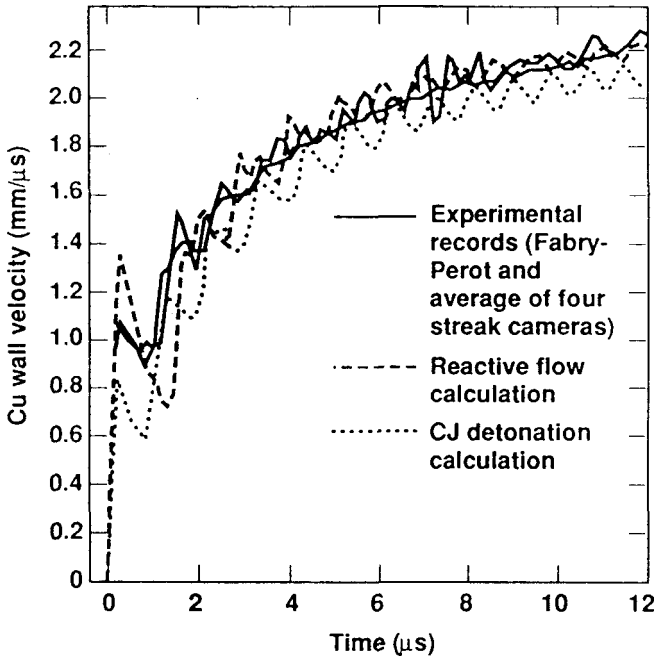

FIGURE 3. COMPARISON OF AVERAGE EXPERIMENTAL RECORDS AND CALCULATIONS OF THE COPPER CYLINDER WALL VELOCITY PRODUCED BY DETONATING RX-25-BF AND RX-25-BP.

with 25.5 mm of RX-25-BF, BP or BQ with and without LX-10 boosters. The measured interface velocities are shown in Fig. 5, along with the corresponding reactive flow and CJ detonation calculations. The reactive flow parameters for RX-25-BF in Table 1 yield excellent agreement with the measured von Neumann spike and subsequent reaction time of approximately 0.3 μs in Fig. 3 and agrees with the CJ detonation calculation at times longer than 0.5 μs. The slower decrease in particle velocity in the experimental records of Fig. 5 as compared to the calculations in the 0.4–0.6 μs region implies either that a relatively slow, weak exothermic reaction is occurring in this time frame or that the product equation of state is slightly incorrect at these pressures. Nevertheless, this ZND reactive flow model is an excellent one-dimensional representation of the fully developed detonation wave in RX-25-BF. The agreement between the experimental records and the reactive flow calculation during the first 0.1–0.15 μs of Fig. 5 also justifies the use of the HMX reaction rates for the initial 38% of the reaction in RX-25-BF.

The critical diameter-detonation velocity experiments described earlier measure the response of the detonation reaction rates to rarefaction waves propagating inward from the unconfined charge boundaries. They also represent good tests of the two-dimensional

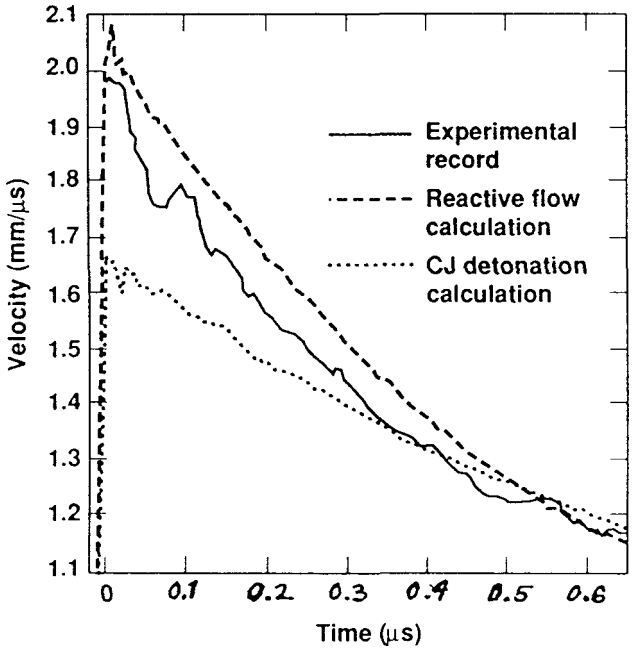

FIGURE 4. EXPLOSIVE-LIF WINDOW INTERFACE VELOCITY HISTORIES PRODUCED BY 1.26 CM OF DETONATING RX-25-BF AND RX-25-BP.

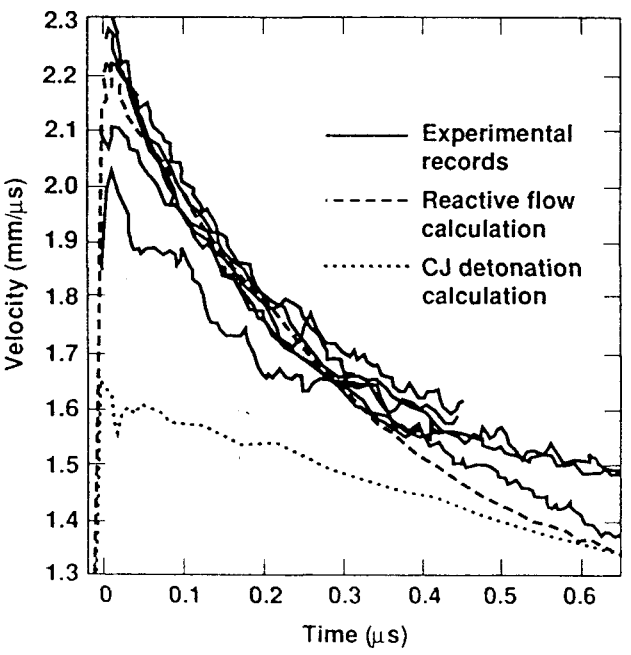

FIGURE 5. EXPLOSIVE-LIF WINDOW INTERFACE VELOCITY HISTORIES PRODUCED BY 2.55 CM OF DETONATING RX-25-BF AND RX-25-BP.

reactive flow model. The entire experiment is modeled in DYNA2D[20] with 50 zones per centimeter in the tetryl booster (CJ detonation), LX-17 booster (reactive flow[13]) and RX-25-BP (reactive flow). Figures 6 and 7 show the calculated pressure and fraction reacted contours for the detonating 12.7 mm diameter (6.35 mm radius) RX-25-BP charge near the end of the 6.36 cm long run distance. After an initial slight overdrive to 7.13 mm/μs, the detonation velocity in this RX-25-BP charge measured by the final three pins was 6.98 mm/μs. The calculated detonation velocity for the RX-25-BP reactive flow parameters listed in Table 1 is 6.75 ± 0.09 mm/μs. Figure 6 shows that this calculated detonation wave front exhibits considerable curvature but its peak pressure approaches the one-dimensional CJ pressure of 28 GPa. Figure 7 shows that 90% of the reaction is completed within 0.2 cm (or 0.3 μs) of the shock front.

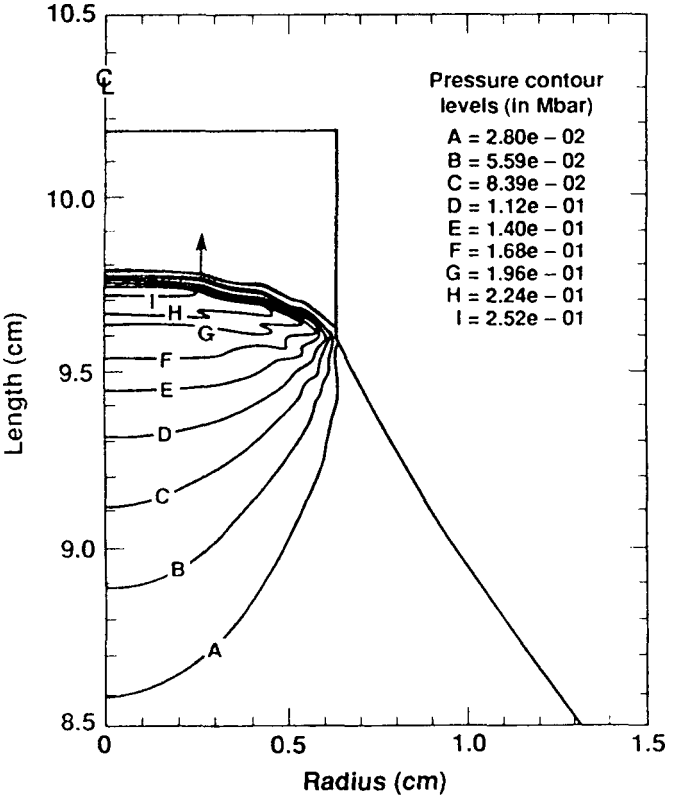

FIGURE 6. CALCULATED PRESSURE CONTOURS FOR RX-25-BF DETONATING IN A 12.7 MM DIAMETER CYLINDRICAL CHARGE.

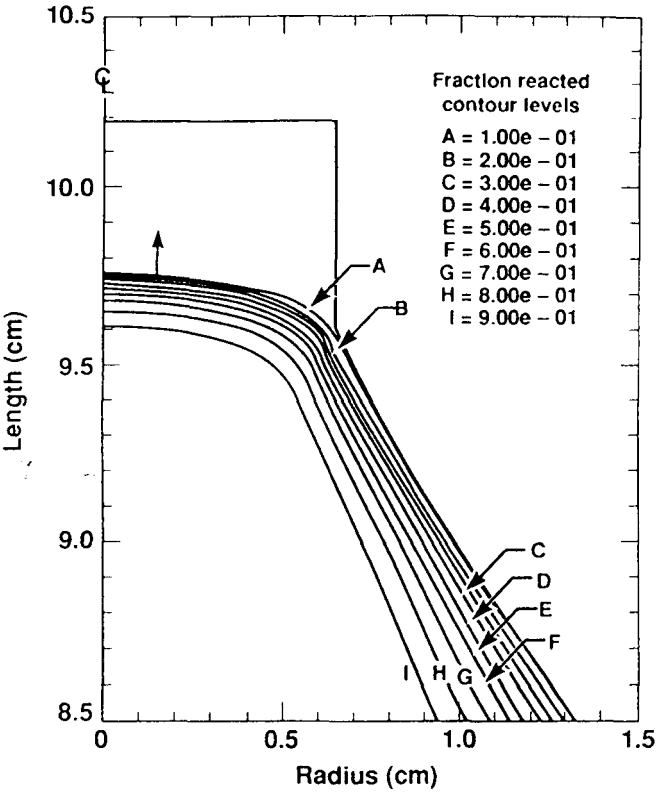

FIGURE 7. CALCULATED FRACTION REACTED CONTOURS FOR RX-25-BP DETONATING IN A 12.7 MM DIAMETER CYLINDRICAL CHARGE.

Figures 8 and 9 show the calculated pressure and fraction reacted contours for the detonating 6.4 mm diameter (3.2 mm radius) RX-25-BP charge at the end of the 3.20 cm long run distance. The measured detonation velocity for this experiment was 6.70 mm/μs, while the calculated detonation velocity was 6.14 ± 0.14 mm/μs. Figure 8 shows a very weak, curved detonation wave with a peak pressure of only 16 GPa and Fig. 9 shows that the 90% reacted contour is approximately 0.5 cm (or 0.8 μs) behind the shock front on the charge axis. While this reactive flow model accurately simulates the 12.7 mm diameter detonation wave of RX-25-BP, it appears to predict too great a pressure and detonation velocity deficit at 6.35 mm diameter, which is very close to the failure diameter of RX-25-BP. Additional detonation velocity-charge diameter and embedded pressure gauge experiments in the region of reaction failure are required for further model refinement.

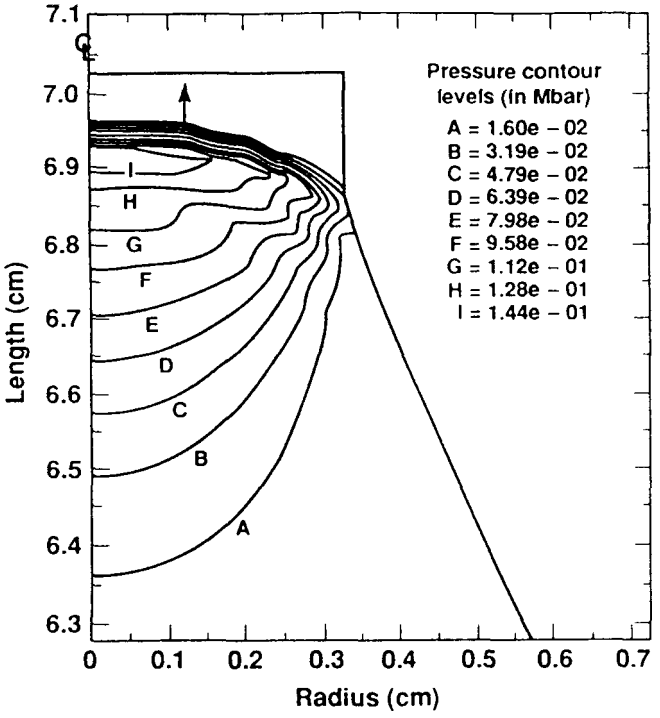

FIGURE 8. CALCULATED PRESSURE CONTOURS FOR RX-25-BP DETONATING IN A 6.35 MM DIAMETER CYLINDRICAL CHARGE.

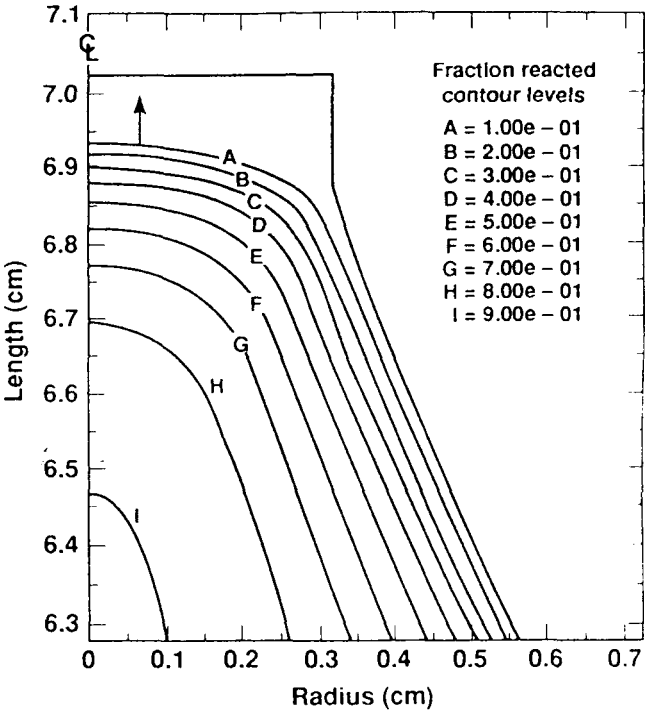

FIGURE 9. CALCULATED FRACTION REACTED CONTOURS FOR RX-25-BP DETONATING IN A 6.35 MM DIAMETER CYLINDRICAL CHARGE.

CONCLUSIONS

One- and two-dimensional experiments and reactive flow hydrodynamic calculations for detonating RX-25-BH (19% HMX/47% AP/30% ZrH_2/4% estane) and RX-25-BF (38% HMX/36% AP/22% ZrH_2/4% estane) have yielded sufficient information to develop a computer model which can be used to evaluate these composite explosives in a wide variety of metal acceleration applications. In this model the HMX reaction rates determined for other HMX-based explosives are used for the first 19% (RX-25-BH) or 38% (RX-25-BF) of reaction. The remainder of the chemical reactions (AP and ZrH_2 decomposition and any subsequent diffusion reactions between the sets of reaction products) are described by one pressure dependent term in the reaction rate equation. Further experimentation on the equations of state and decomposition rates of the individual components ZrH_2 and AP and the diffusion of their reaction products is required to model more completely the complex reactive flow produced by the detonation of these and other composite explosives.

REFERENCES

1. J. W. Kury, H. C. Hornig, E. L. Lee, J. L. McDonnel, D. L. Ornellas, M. Finger, F. M. Strange, and M. L. Wilkins, Fourth Symposium (International) on Detonation, Office of Naval Research, ACR-126, 1965, p. 3.

2. M. Finger, H. C. Hornig, E. L. Lee, and J. W. Kury, Fifth Symposium (International) on Detonation, Office of Naval Research, ACR-184, 1970, p. 137.

3. M. Finger, E. Lee, F. H. Helm, B. Hayes, H. Hornig, R. McGuire, and M. Kahara, Sixth Symposium (International) on Detonation, Office of Naval Research, 1976, p. 710.

4. M. Finger, F. Helm, E. Lee, R. Boat, H. Cheung, J. Walton, B. Hayes, and L. Penn, Sixth Symposium (International) on Detonation, p. 729.

5. R. R. McGuire, D. L. Ornellas, F. H. Helm, C. L. Coon, and M. Finger, Seventh Symposium (International) on Detonation, Naval Surface Weapons Center, NSWC MP 82-334, 1981, p. 940.

6. R. R. McGuire and M. Finger, Eighth Symposium (International) on Detonation, Naval Surface Weapons Center, NSWC MP 86-194, 1985, p. 1018.

7. R. M. Doherty, J. M. Short, and M. J. Kamlet, Combustion and Flame, Vol. 76, 1989, p. 297.

8. R. M. Doherty, J. M. Short, I. B. Akst, and M. J. Kamlet, Combustion and Flame, Vol. 76, 1989, p. 369.

9. E. L. Lee, and C. M. Tarver, Phys. Fluids, Vol. 23, 1980, p. 2362.

10. B. Hayes and C. M. Tarver, Seventh Symposium (International) on Detonation, Naval Surface Weapons Center, NSWC MP 82-334, 1981, p. 1029.

11. C. M. Tarver, N. L. Parker, H. G. Palmer, B. Hayes, and L. M. Erickson, J. Energetic Materials, Vol. 1, 1983, p. 213.

12. S. A. Sheffield, D. D. Blomquist, and C. M. Tarver, J. Chem. Phys. Vol. 80, 1984, p. 3831.

13. K. Bahl, G. Bloom, L. Erickson, R. Lee, C. Tarver, W. Von Holle, and R. Weingart, Eighth Symposium (International) on Detonation, Naval Surface Weapons Center, NSWC MP 86-194, 1985, p. 1045.

14. C. M. Tarver, R. D. Breithaupt, and J. W. Kury, International Symposium on Pyrotechnics and Explosives, Beijing, China, 1987, p. 692.

15. L. G. Green, C. M. Tarver, and D. J. Erskine, paper presented at this Symposium.

16. P. A. Urtiew, L. M. Erickson, D. F. Aldis, and C. M. Tarver, paper presented at this Symposium.

17. C. M. Tarver, J. O. Hallquist, and L. M. Erickson, Eighth Symposium (International) on Detonation, Naval Surface Weapons Center, NSWC MP 86-194, 1985, p. 951.

18. C. M. Tarver and L. G. Green, paper presented at this Symposium.

19. E. Lee, D. Breithaupt, C. McMillian, N. Parker, J. Kury, C. Tarver, W. Quirk, and J. Walton, Eighth Symposium (International) on Detonation, Naval Surface Weapons Center, NSWC MP 86-194, 1985, p. 613.

20. J. O. Hallquist, User's Manual for DYNA2D, UCID-18756 Rev. 3, 1986, Lawrence Livermore National Laboratory, Livermore, California.

21. C. M. Tarver, L. M. Erickson, and N. L. Parker, Shock Waves in Condensed Matter—1983, edited by J. R. Asay, R. A. Graham, and G. K. Straub, Elsevier Science Publishers B.V., 1984, p. 609.

22. W. L. Seitz, H. L. Stacy, and J. Wackerle, Eighth Symposium (International) on Detonation, Naval Surface Weapons Center, NSWC MP 86-194, 1985, p. 123.